AIP | The Journal of Chemical Physics

Orientational relaxations in solid (1,1,2,2)tetrachloroethane

P. Tripathi, E. Mitsari, M. Romanini, P. Serra, J. Ll. Tamarit, M. Zuriaga, and R. Macovez

Citation: The Journal of Chemical Physics **144**, 164505 (2016); doi: 10.1063/1.4947477
View online: http://dx.doi.org/10.1063/1.4947477
View Table of Contents: http://scitation.aip.org/content/aip/journal/jcp/144/16?ver=pdfcov
Published by the AIP Publishing

Orientational relaxations in solid (1,1,2,2)tetrachloroethane

P. Tripathi,[1] E. Mitsari,[1] M. Romanini,[1] P. Serra,[2] J. Ll. Tamarit,[1] M. Zuriaga,[2] and R. Macovez[1,a)]

[1]*Grup de Caracterització de Materials, Departament de Física i Enginyeria Nuclear, Universitat Politècnica de Catalunya, ETSEIB, Diagonal 647, 08028 Barcelona, Spain*

[2]*Facultad de Matemática, Astronomía y Física, Universidad Nacional de Córdoba and IFEG-CONICET, Ciudad Universitaria, X5016LAE Córdoba, Argentina*

(Received 9 February 2016; accepted 11 April 2016; published online 27 April 2016)

We employ dielectric spectroscopy and molecular dynamic simulations to investigate the dipolar dynamics in the orientationally disordered solid phase of (1,1,2,2)tetrachloroethane. Three distinct orientational dynamics are observed as separate dielectric loss features, all characterized by a simply activated temperature dependence. The slower process, associated to a glassy transition at 156 ± 1 K, corresponds to a cooperative motion by which each molecule rotates by 180° around the molecular symmetry axis through an intermediate state in which the symmetry axis is oriented roughly orthogonally to the initial and final states. Of the other two dipolar relaxations, the intermediate one is the Johari-Goldstein precursor relaxation of the cooperative dynamics, while the fastest process corresponds to an orientational fluctuation of single molecules into a higher-energy orientation. The Kirkwood correlation factor of the cooperative relaxation is of the order of one tenth, indicating that the molecular dipoles maintain on average a strong antiparallel alignment during their collective motion. These findings show that the combination of dielectric spectroscopy and molecular simulations allows studying in great detail the orientational dynamics in molecular solids. *Published by AIP Publishing.* [http://dx.doi.org/10.1063/1.4947477]

INTRODUCTION

While conventional (atomic) solids are made of atomic constituents with only translational degrees of freedom, so that their structure is totally determined by translation symmetry and fundamental excitations are vibrational in character, in molecular solids, the constituent molecules possess also orientational (as well as internal) degrees of freedom, which lead to a richer variety of possible solid phases and to the existence of rotational excitations such as librations and orientational relaxations. A molecular solid can display complete translational and rotational order, as in a molecular crystal, or complete rototranslational disorder, as in a molecular glass. In between these two extremes, molecular solids also display phases (known as "mesophases") that have no counterpart in atomic solids: for example, phases in which all molecules have the same or similar orientation, but no translational order (liquid crystals), or phases in which the molecules' average centres of mass occupy lattice positions while their orientations are disordered [orientationally disordered (OD) solids, a prominent example of which are rotator phases or plastic crystals]. Finally, molecules possessing distinct isomers may be present in the same phase in different isomeric forms (conformationally disordered solids).

Orientationally disordered (OD) phases are generally formed by relatively small globular molecules such as derivatives of methane,[1–3] neopentane,[4] adamantane[5] or fullerene,[6] or by small linear ones such as ethane derivatives[7–9] and dinitriles.[10] OD solids exhibit many of the phenomenological features of glass formers, displaying in particular a cooperative rotational motion, called α relaxation, that undergoes a continuous, dramatic slow-down upon cooling,[11,12] leading in some cases to a glass-like transition associated with rotational freezing.[13,14] Contrary to structural glasses, which do not exhibit any long-range order, OD phases are characterized by a translationally ordered structure and can therefore be more thoroughly characterized with the help of methods that exploit the translational symmetry such as Bragg diffraction, lattice models, or solid-state nuclear magnetic resonance spectroscopy. Even more importantly, since as mentioned, OD phases are generally formed by molecular species with a simple structure and low number of atoms, solid-state molecular simulations are computationally affordable and can be performed with a relatively large number of molecules. This advantage allows an exact identification of the cooperative and non-cooperative molecular motions taking place in an OD phase, as we show here for the case of a chemically very simple molecule, namely, (1,1,2,2)tetrachloroethane $C_2H_2Cl_4$ (hereafter TCE).

TCE is known to exist in three molecular conformers (*gauche*$^+$, *gauche*$^-$, and *trans*) depending on the phase and to display a rich phase diagram depending on temperature, pressure, and thermal treatment.[15,16] Under ambient conditions, TCE is liquid and consists both of *gauche* and *trans* isomers, with the *gauche* conformers being slightly more stable than the *trans* one.[17] At ambient pressure, the thermodynamically stable phase of TCE below 231 K is orthorhombic ($P2_12_12_1$, $Z = 8$, $Z' = 2$), with all the molecules

a)Author to whom correspondence should be addressed. Electronic mail: roberto.macovez@upc.edu

in the *gauche*$^+$ conformation.[15,16] A metastable solid form is known, which is obtained by recrystallization upon heating the structural glass obtained by rapid cooling of the liquid, and which is observed in a limited temperature range; this metastable phase was found to be monoclinic ($P2_1/c$) with Z = 8 molecules in the unit cell and Z′ = 2 in the asymmetric unit, with both *gauche*$^+$ and *gauche*$^-$ conformers coexisting in the asymmetric unit.[16] Finally, at high pressures (above 0.5 GPa at room temperature), the stable phase is a monoclinic phase ($P2_1/c$, Z = 2, Z′ = 0.5) in which all molecules are in the *trans* conformation.[15]

Molecular reorientational dynamics were reported in the orthorhombic phase consisting only of *gauche*$^+$ conformers, where a full assignment of the dynamics was so far not possible,[18] and in the high-pressure monoclinic phase, where the *trans* conformers undergo rotational motions in which the C–C bond changes its spatial orientation while the chlorine atoms interchange their positions in the crystal structure (in what could be termed a "positional-exchange" reorientation).[19] In this contribution, we focus on the orthorhombic phase stable at ambient pressure. By employing temperature-dependent dielectric spectroscopy, we identify three different dipolar relaxation dynamics. Comparison with molecular dynamics simulations allows assigning unambiguously each relaxation to a specific molecular reorientation in the solid matrix. We identify in particular a cooperative dipolar relaxation associated with a reorientational dynamics in which the initial and final molecular orientations are the same. We find that this cooperative motion has a non-cooperative precursor relaxation. We also observe a fast dynamics associated with molecular fluctuations involving the population of higher-energy (non-equilibrium) orientations. These results show that mesophases of even simple molecules can exhibit very rich orientational dynamics.

METHODS

Dielectric spectroscopy

Dielectric spectroscopy probes the complex permittivity of a sample as a function of frequency. In dielectric measurements, an ac electric field is applied to a parallel-plate capacitor formed by a homogeneous sample sandwiched between two metal disks. Using the known surface area and thickness of the dielectric sample, the complex permittivity is directly extracted from the complex impedance of the capacitor cell, which is measured with an impedance analyzer. For the dielectric measurements, liquid (1,1,2,2)tetrachloroethane was inserted inside a home-made stainless steel parallel-plate capacitor, especially designed for liquid samples, with the two plates separated by needle-like cylindrical silica spacers of 50 μm diameter. The capacitor was then loaded within a nitrogen-gas flow cryostat for temperature control. To obtain the orthorhombic phase of (1,1,2,2)tetrachloroethane, the sample was cooled down to 130 K and then warmed up to below 230 K to avoid melting of the solid phase,[16] and isothermal spectra were then taken always below this temperature.

Isothermal dielectric spectra were acquired using a Novocontrol Alpha analyzer in the frequency (f) range between 10^{-2} and 5×10^6 Hz. The imaginary part $\varepsilon''(f)$ of the complex permittivity, called dielectric loss spectrum, carries information on the dipolar molecular dynamics processes taking place in the sample, with processes of distinct origin appearing in different characteristic frequency ranges. At low frequency and high-enough temperatures, the dielectric loss is dominated by Joule losses associated with charge conduction, which give rise to a loss background proportional to reciprocal frequency corresponding to the low-frequency dc plateau of the ac conductivity spectrum $\sigma'(f) = 2\pi f \varepsilon_0 \varepsilon''(f)$. At higher frequency, the loss spectrum displayed different bump-like features corresponding to distinct reorientational processes. Each feature was modeled as the imaginary part of the complex Cole-Cole function whose analytic expression is[20,21]

$$\varepsilon_{CC}(f) = \varepsilon_\infty + \frac{\Delta\varepsilon}{1 + (i2\pi f\tau)^d}. \quad (1)$$

Here, $\Delta\varepsilon = \varepsilon_s - \varepsilon_\infty$ is the dielectric strength, ε_∞ and ε_s being the high-frequency and static low-frequency limits of the real permittivity. The parameter d, called Cole–Cole exponent, lies in the range from 0 to 1 and is related to the width of the relaxation time distribution; finally, τ is the characteristic time at which the dielectric loss of the given relaxation process is maximum. Each dielectric loss spectrum was fitted as the imaginary part of one or more Cole-Cole functions, superposed to a background, proportional to reciprocal frequency that mimicked the conductivity contribution, when this was visible in the spectrum, or else the high-frequency tail of a relaxation peaked at lower frequency than experimentally accessible.

A. Molecular simulations

Molecular dynamics simulations of (1,1,2,2)tetrachloroethane were performed in the NVT ensemble. Rigid molecules were considered in *gauche*$^+$ configuration and the intramolecular parameters used were obtained from previously published X-ray diffraction data in Ref. 16. The intermolecular interactions were described by Lennard-Jones (L-J) and Coulombic potentials[22–25] (see Ref. 18 for more details).

NVT simulations were performed using the Gromacs v5.0.2 package,[26] using a leap-frog algorithm with a time step of 0.0005 ps and a velocity rescale thermostat with a time constant of 2 ps. The experimental volume and the perfect crystalline structure determined by X-ray diffraction were used as initial configuration.[15,16] The system was formed by 800 molecules (6400 atoms), and some tests with a larger system of 6400 molecules (51 200 atoms) were done in order to discard finite-size effects. Runs of 20 000 ps were done, taking averages over the last 5000 ps. Some very large runs (300 000 ps) were made for some temperatures in order to corroborate the shorter time results.

We also performed a couple of NVT simulations with non-rigid molecules in order to discard *gauche-trans* conformational jumps and to calculate the dynamic correlation

between molecular orientations. In these simulations, we included harmonic atom-atom forces, three-body harmonic angle potentials, and a four-body dihedral Ryckaert-Bellemans potential allowing torsion of the molecule around the C–C bond.[27–29] A molecular dynamics simulation was performed during 150 000 ps for the largest system (6400 molecules). We used this run in order to calculate the Kirkwood correlation factor.

RESULTS AND DISCUSSION

Fig. 1 shows the isothermal dielectric loss spectra $\varepsilon''(f)$ of the orthorhombic phase of TCE, displayed in two separate temperature ranges between 221 and 145 K. At high temperature (Fig. 1(a)), the loss spectra exhibit a low-frequency background proportional to reciprocal frequency, which stems from the dc conductivity contribution. This is confirmed by the shape of the ac conductivity spectrum, shown in the inset to the same panel for the temperature of 221.2 K, which below ~1 Hz exhibits a low-frequency plateau corresponding to the σ_{dc} value. In the loss spectra of Fig. 1(a), two features are discernible on top of the dc-conductivity background, labeled as α and β. At lower temperature (Fig. 1(b)), a third feature is observed (at higher frequency than both α and β processes), labeled as γ. In the spectra of Fig. 1(b), the maximum of the α loss is outside the depicted frequency range, so that the low-frequency background visible in the spectra corresponds to the high-frequency tail of such loss.

The real permittivity spectra $\varepsilon'(f)$ (shown in the inset in Fig. 1(b) for the temperature of 193.2 K) are monotonically decreasing functions of frequency, as expected. At low frequency, instead of reaching a plateau value corresponding to the static permittivity ε_s, the spectra exhibit a steep increase with decreasing frequency (likely due to a conductivity or polarization effect). Hence, the value of ε_s cannot be extracted directly from the real permittivity data.

It is remarkable that a simple, rigid molecule like the *gauche*$^+$ conformer of TCE exhibits three distinct relaxation processes. In order to determine the origin of each relaxation process, we carried out a detailed quantitative analysis of the spectra based on the fitting procedure detailed in the Methods section, with each relaxation feature modeled as a Cole-Cole function. The obtained characteristic times τ_α, τ_β, and τ_γ of the three relaxations are shown together as Arrhenius plots in Fig. 2. It may be observed that the temperature dependence of all three processes follows a simply activated (Arrhenius) behavior, given by

$$\tau = \tau_0 \exp\left(E_a/k_B T\right). \tag{2}$$

Here, the prefactor τ_0 is the value of the relaxation time in the limit of very high temperature, k_B is the Boltzmann constant, and E_a is the activation energy, which represents the energy barrier for the process.[30]

The fitting procedure also yielded the dielectric strength ($\Delta\varepsilon$) for each dynamic process. It may be observed from Fig. 1(a) that the strength of the α feature appears to increase slightly with increasing temperature. This is confirmed by our

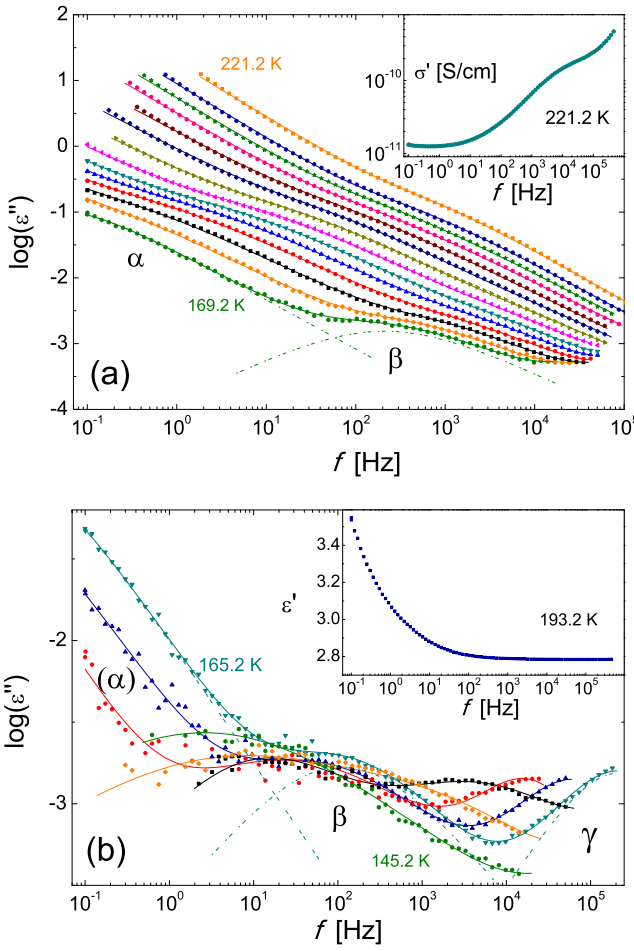

FIG. 1. Dielectric loss spectra of orthorhombic TCE between 221.2 and 169.2 K (a) and between 165.2 and 145.2 K (b), every 4 K, and corresponding fits (continuous lines). Three molecular dynamic processes are visible, labeled, respectively, as α, β, and γ. Insets: logarithmic ac conductivity spectrum $\sigma'(f)$ at 221.2 K (a) and permittivity spectrum $\varepsilon'(f)$ at 193.2 K (b).

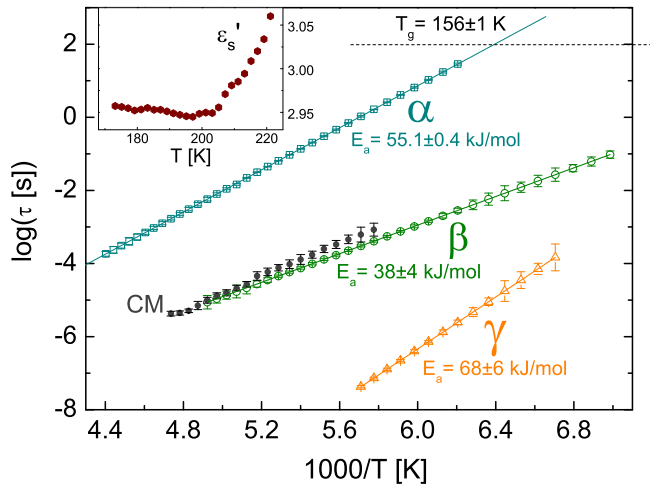

FIG. 2. Arrhenius plot of the characteristic times of all three relaxation processes (α, β, and γ) observed in TCE (open markers with error bars). Continuous lines are fits with the Arrhenius Eq. (2), and the dashed line indicates the glass transition temperature of the α process. Filled circles with error bars indicate the predicted relaxation time of the Johari-Goldstein precursor according to the Coupling Model (CM) (Eq. (3), see the text for more details). Inset: plot of the static permittivity ε_s as a function of temperature.

fitting results; to better visualize such increase, in the inset to Fig. 2, we plot the static permittivity (ε_s) of solid TCE as a function of temperature. The value of ε_s was determined as $\varepsilon_s = \varepsilon_\infty + \Delta\varepsilon_\alpha + \Delta\varepsilon_\beta$, where $\Delta\varepsilon_\alpha$ (respectively, $\Delta\varepsilon_\beta$) is the dielectric strength of the α (respectively, β) relaxation, and ε_∞ is the value of the real permittivity at frequency higher than the characteristic frequency of the β relaxation (and lower than the γ relaxation), where a plateau is visible in the $\varepsilon'(f)$ spectra (see inset of Fig. 1(b)). Given that $\Delta\varepsilon_\alpha$ is roughly two orders of magnitude greater than $\Delta\varepsilon_\beta$ and that ε_∞ is basically constant, the temperature dependence of the static permittivity follows that of the dielectric strength of the primary relaxation.

It may be observed in the inset of Fig. 2 that ε_s initially decreases slowly with increasing temperature, but upon approaching the melting point at 231 K,[15] it exhibits a steep increase. The initial decrease is consistent with the general expectation that $\Delta\varepsilon_\alpha$ and ε_s decrease with increasing temperature because the alignment of mobile molecular dipoles with the applied field is hampered at high temperature by thermal motions. The steep increase close to the melting point, although inconsistent with this general trend, is however in agreement with the results obtained in a similar system, namely, (1,1,2)trichloroethane,[31] where it was reported that the dynamic orientational disorder is more pronounced close to the melting while it is almost absent at lower temperature. (1,1,2,2)tetrachloroethane appears therefore to display a similar behavior, with more pronounced (dynamic) orientational disorder close to the melting point.

The characteristic times τ_α obtained by our fitting procedure match roughly with those reported in a recent nuclear quadrupole resonance study on the orthorhombic phase of TCE.[18] This slowest relaxation process (α) corresponds to the cooperative motion associated with the glass-like freezing of the collective molecular motion (i.e., with a glassy transition).[18] The observation of the same relaxation by means of dielectric spectroscopy implies that it is dipolar in character, i.e., it involves a change in the macroscopic polarization of the sample under the applied ac field. It is clear from Fig. 1(a) that the molecular motion corresponding to the α relaxation can be frozen without transition to a more ordered crystalline phase, i.e., that a glassy state is reached.

The Arrhenius parameters for the α relaxation obtained from the fit of the corresponding Arrhenius plot with Eq. (2) were $E_a = 55.1 \pm 0.4$ kJ/mol and $\log(\tau_0/[\mathrm{s}]) = -16.4 \pm 0.2$. The result for τ_0 is in the typical range of values for glass-forming materials.[30] The activation energy is somewhat higher than that reported for deuterated TCE (41 kJ/mol).[18] The glass transition temperature was calculated as the temperature at which the Arrhenius Eq. (2) gave a value of τ_α equal to 100 s. The obtained value, $T_g = 156 \pm 1$ K, is close to the glass transition temperature of supercooled liquid TCE (153 K), as already pointed out in Ref. 18 for deuterated TCE.

Starting from the fitting parameters of the α relaxation feature, one may employ the so-called Coupling Model (CM)[32] to calculate the relaxation time τ_{CM} of the precursor relaxation associated with the glass transition dynamics, i.e., the characteristic time of the (single-molecule) Johari-Goldstein relaxation.[33,34] According to the CM, the relaxation time τ_{CM} of the precursor relaxation should be related with that of the primary process (τ_α) as

$$\log(\tau_{CM}) = (1 - \beta_{KWW}) \log(t_c) + \beta_{KWW} \log(\tau_\alpha). \quad (3)$$

Here, t_c is a crossover time whose typical value is 2×10^{-12} s for both molecular and polymeric glass formers,[32,35] and β_{KWW} is the exponent of the stretched exponential function that describes the α spectral feature in the time domain. For the Cole-Cole exponent d of the function employed to fit the α feature (see Methods section), the value of β_{KWW} can be accurately estimated as $\beta_{KWW} \cong d^{1/1.23}$.[36,37] The theoretical precursor time τ_{CM} calculated using Eq. (3) is shown in Fig. 2 together with the experimental values for all three relaxation times. It can be observed that τ_{CM} matches rather closely the experimental values for τ_β. Moreover, if the simply activated behaviors of both the α and β are extrapolated to high temperatures, they are observed to intersect at high temperature (~500 K), where both characteristic times are roughly equal and given by $\log(\tau_\alpha) \approx \log(\tau_\beta) \approx -11$. We can therefore conclude that the secondary β relaxation is the precursor relaxation associated with the primary relaxation.

Visual inspection of Fig. 1(b) reveals that the spectral position of the γ feature varies more rapidly with temperature than the β process. This is confirmed by the Arrhenius plot of Fig. 2, where it is observed that the γ relaxation has also higher activation energy than the α process. Given that we already identified the β relaxation as the precursor of the primary relaxation, the γ process is not a precursor single-molecule relaxation; moreover, it also cannot be an intramolecular relaxation, because the *gauche*$^+$ conformer is rigid and previous studies have already ruled out the existence of conformational fluctuations in the orthorhombic phase.[15,16,18] In order to identify the exact microscopic origin of the α and γ relaxations, we carried out detailed molecular dynamics simulations in this phase. The molecular structure of the *gauche*$^+$ conformer present in orthorhombic TCE possesses a C_2 symmetry axis orthogonal to the C–C bond and midway between the two carbon atoms. Due to the different electron affinity of hydrogen and chlorine species, the TCE molecule is dipolar, and by symmetry, its dipole moment is parallel to the C_2 axis (orthogonal to the C–C bond), oriented from the chlorine-rich to the hydrogen-rich region of the molecule.

It was pointed out already in Ref. 18 that the only molecular dynamics present in orthorhombic TCE are two, namely, reorientational motions of the molecule between equivalent ground-state orientations (180° flips around the molecular symmetry axis) and between the ground-state orientation and a non-equilibrium orientation.

The first dynamic process is in fact a positional exchange of C, H, and Cl atoms in the molecule, associated with a 180° rotation about the molecular symmetry axis. This motion is depicted in Fig. 3, where the coordinates of two carbon (a) and two chlorine (b) atoms of a given molecule are shown during one and a half nanoseconds of simulation covering such a reorientation process. The initial and final coordinates show clearly the exchange between the two carbons and the two shown chlorine atoms. Although the initial and final states are identical (they correspond in fact to a rotation by 0° or 180° around the C_2 molecular symmetry axis), during

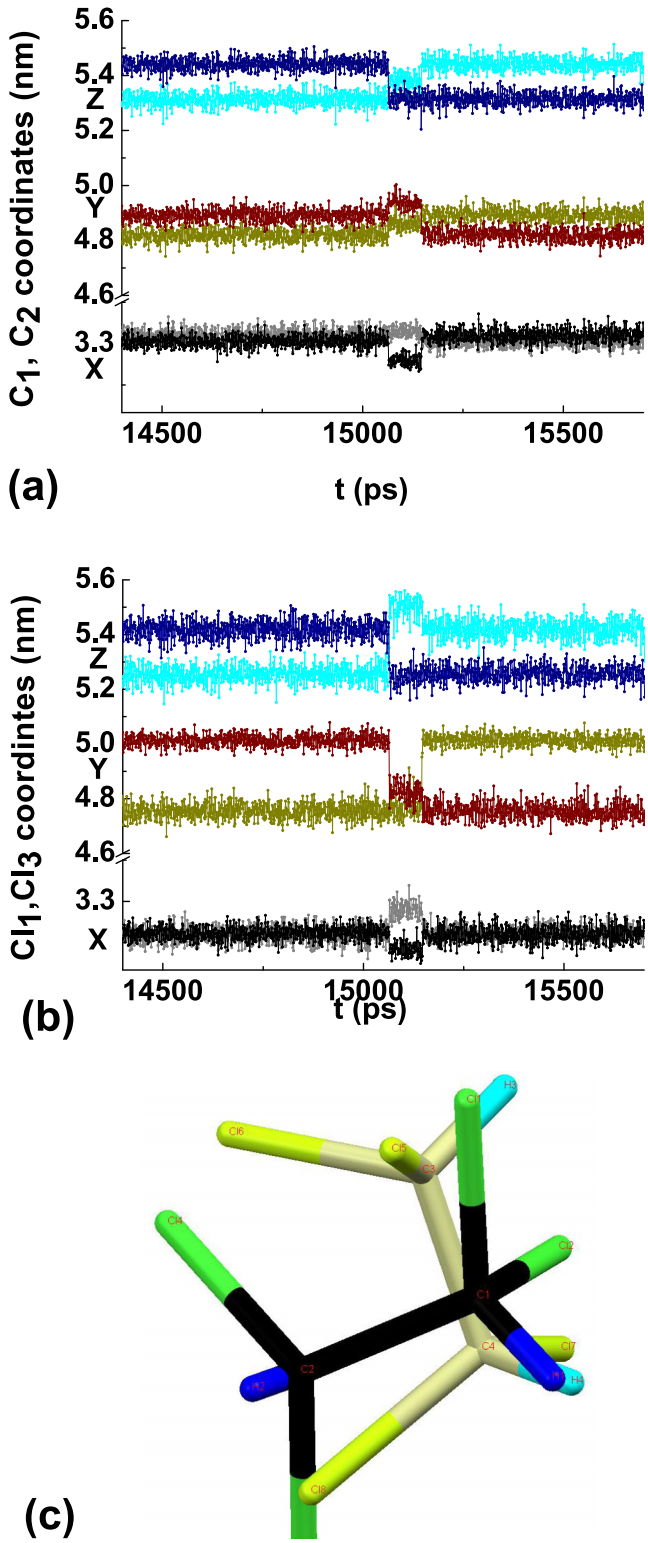

FIG. 3. Carbon (a) and selected chlorine (b) coordinates of a TCE molecule during 1.5 ns of NVT molecular dynamics simulations covering the 180° flip about the molecular symmetry axis. (c) Relative orientation of the intermediate state attained during such reorientational motion (yellow) with respect to the initial/final state (black).

the transition between the two states, the molecule passes through an intermediate state with a different direction of the symmetry axis, shown in Fig. 3(c). This entails that such dynamics is visible with dielectric spectroscopy (while a rigid rotation around the symmetry axis would not be). We notice that 180° rotations represent the typical dynamic motions of elongated molecules in the liquid phase (see, e.g., Ref. 38 and references therein); here, however, the rotational dynamics occurs in the solid phase, where steric hindrance is enhanced.

The other dynamic process is the temporary population of a higher-energy state. The relative orientation of the initial (ground) and final (higher-energy) states is depicted in Fig. 4(c), while the other panels of Fig. 4 describe the positions of the two carbons (a) and two chlorines (b) during 10 ns of simulation covering such a back-and-forth reorientation. It

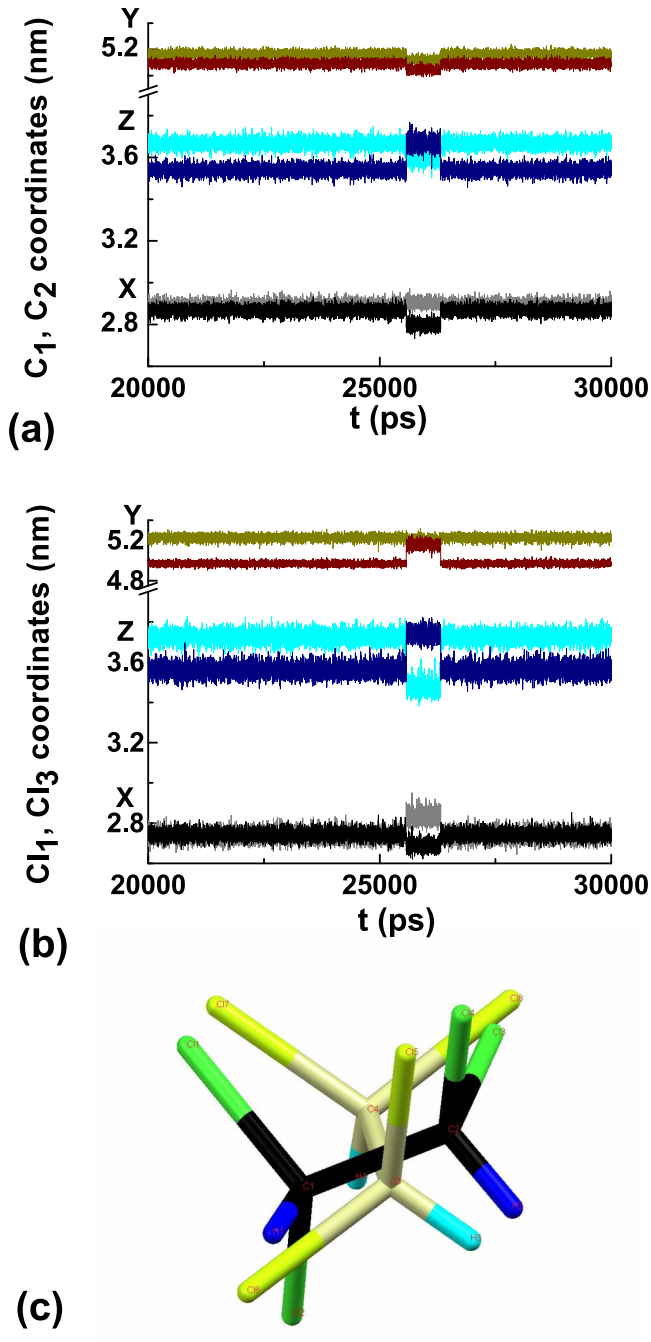

FIG. 4. Carbon (a) and selected chlorine (b) coordinates of a TCE molecule during 10 ns of NVT molecular dynamics simulations covering a dynamic transition to and from a high-energy orientational state. (c) Relative orientations of a TCE molecule in the high-energy orientation (yellow) as compared to the ground-state orientation (black).

may be observed comparing Figs. 3(b) and 4(b) that the positions of the chlorine atoms in the intermediate step are different in the two dynamic processes. Since the possible molecular orientations in chloroethanes are determined to a large extent by the steric hindrance between the bulky chlorines atoms,[31] the two intermediate orientations shown in Figs. 3(c) and 4(c) correspond to states of different energy.

Since a collective fluctuation involving a large population of molecules in the higher-energy state is energetically forbidden, we assign the γ process to the back-and-forth dynamics of Fig. 4(c), and the α relaxation to a cooperative reorientation involving the positional exchange of Fig. 3(c). This assignment is consistent with the observed activation energies, as it is likely that a dynamic process between two states of different energy involves a higher energy barrier than a process between two equivalent states of same energy.

The β relaxation is therefore the precursor relaxation associated with the cooperative 180° reorientational flips. The situation is reminiscent of the behavior of a solid phase of 2-adamantanone, which displays both a cooperative and a precursor relaxation associated with large-angle reorientational jumps.[5] However, contrary to the adamantanone case, the initial and final states of the α relaxation are here indistinguishable. To the best of our knowledge, ours is the first experimental observation by dielectric spectroscopy of a fixed-angle reorientation where the initial and final states coincide. It is also the first time that a precursor relaxation is reported for such peculiar dynamics. This finding corroborates the idea that the Johari-Goldstein precursor relaxation is a fundamental property of glass-forming materials, regardless on the type of disorder they display[39] (a Johari Goldstein precursor relaxation is also observed, for example, in molecular dynamic simulations of the 180° flips of elongated molecules in the liquid state[38]).

It is interesting to analyze in more detail the static permittivity and dielectric strength of the α relaxation. The dielectric strength of a cooperative process can be written, according to the Kirkwood-Fröhlich equation,[30] as

$$\Delta\epsilon = \epsilon_s - \epsilon_{hf} = \frac{g}{3\epsilon_0}\frac{\epsilon_s(\epsilon_{hf}+2)}{3(2\epsilon_s+\epsilon_{hf})}\frac{\mu^2}{k_BT}\frac{N}{V}. \quad (4)$$

In this expression, ε_s is the static value of the permittivity, already discussed above, while ε_{hf} is the value of ε' at a frequency just above that of the α relaxation (in fact, due to the Kramers–Kronig relation,[30] each relaxation loss corresponds to a separate step-like decrease in the real part of the permittivity). Of the other parameters appearing in Eq. (4), μ is the molecular dipole moment, N/V is the number density of dipoles, and g is the so-called Kirkwood correlation factor[40,41] describing the degree of correlation between the relative orientations of nearest-neighbor dipoles during the reorientation dynamics. The Kirkwood factor can be calculated as

$$g = \frac{\langle \vec{M}\cdot\vec{M}\rangle}{N\mu^2} = \frac{\langle |\vec{M}|^2\rangle}{N\mu^2}. \quad (5)$$

Here, $|\vec{M}|$ is the total electric dipole moment vector of N molecules, and the angle brackets denote a time average. We determined the factor g starting from our simulation data. The total dipole moment $|\vec{M}|$ was calculated for the whole set of molecules used in the simulation (6400), and the average was performed over a relatively large time span. Using the value of the dipole moment provided by our simulation (μ = 2.1 D), the Kirkwood factor at 215 K is found to be equal to 0.06, which is quite low, indicating a largely antiparallel orientation of the molecular dipoles.

To compare this value with the experiment, we first determined the high-frequency value of the real permittivity, ε_{hf}, using the static one and the dielectric strength of the primary relaxation, as $\varepsilon_{hf} = \varepsilon_s - \Delta\varepsilon_\alpha$. This was necessary because it was not possible to reliably separate the contribution of the α and β relaxations to the ε' spectrum. It should be noted that the strength of the β process is two orders of magnitude smaller than that of the α process, so that the contribution of the β process in any of the dielectric quantities in Eq. (4) is very small. To evaluate the other terms in Eq. (5), we used the reported value for the number density of molecules at 215 K, namely, $(1/149.3)\times 10^{30}$ molecules per cubic meter.[15] Using the value of μ given above and the experimental value ε_s = 3.05 of the static permittivity of solid TCE at 215 K at ambient pressure (see inset to Fig. 1(b)), the experimental estimate of the Kirkwood correlation factor is found to be of the order of $g \approx 0.2$. Such value is similar to those reported for OD solids formed by adamantane derivatives.[5,42]

It should be observed that g is zero for a perfectly ordered solid with no net dipole moment; for example, $g = 0$ by symmetry for a perfectly ordered orthorhombic unit cell of TCE, due to the antiparallel alignment of neighboring dipole moments. The value of g (and thus indirectly the value of ε_s) therefore measures the correlation between the next-neighbor orientations of the dipole moments as they rearrange by the α dynamics, since the contribution due to the equilibrium structure vanishes. Eq. (4) is strictly valid only for an isotropic medium such as a supercooled liquid or a translationally ordered cubic phase, so that the experimental value of g can only represent a first approximation for an anisotropic medium such as orthorhombic TCE. It is observed nevertheless that the experimental estimate is of the same order of magnitude as that obtained by molecular dynamics simulation, both differing only by a factor of three. Regardless of its exact numerical value, the fact that g is close to zero not only confirms the cooperative nature of the α relaxation (as $g = 1$ for a gas phase of non-interacting dipoles) but most importantly it implies the tendency of the molecular dipoles to maintain on average their antiparallel alignment during such reorientation process. The cooperative nature of the α process likely results both from steric interactions, which only allow specific relative molecular orientations in a densely packed solid, and from dipole-dipole interactions, which prevent the buildup of macroscopic dipole moments.

CONCLUSIONS

We investigated the dipolar dynamics in the orientationally disordered solid phase of a simple ethane derivative, namely, (1,1,2,2)tetrachloroethane, by means both of dielectric spectroscopy and molecular dynamic simulations.

Unexpectedly, three distinct orientational dynamics are observed in the solid phase, all characterized by a simply activated temperature dependence. The slower (α) process is the cooperative rearrangement of molecules in which each molecule undergoes a rotation by 180° around the molecular symmetry axis and simultaneously a double reorientation of such axis from an initial direction to a roughly orthogonal one and then back to the original molecular orientation and position, in what could be termed a positional-exchange relaxation. The intermediate process (β_{JG}) is the Johari-Goldstein precursor relaxation of the α process, and its relaxation time can be accounted for by the coupling model. Finally, the fastest (γ) dynamics is a non-cooperative process that corresponds to the reorientation of a single molecule in a higher-energy orientation. The glassy transition temperature as determined by the freezing of the cooperative α motions in dielectric spectroscopy is remarkably close to the glass-transition temperature of the supercooled liquid of the same compound; this is even more surprising if one considers that in the liquid two distinct isomeric forms of the molecule are present, while only one of them is present in the solid. The Kirkwood correlation factor for the α relaxation indicates that the molecular dipoles maintain on average a strong antiparallel alignment during their collective reorientational motion, mimicking the equilibrium relative orientations in the unit cell. To the best of our knowledge, this is the first observation by dielectric spectroscopy of a fixed-angle reorientation where the initial and final states coincide, and of the existence of a Johari-Goldstein precursor associated with such a dynamics.

ACKNOWLEDGMENTS

This work has been supported by the Spanish Ministry MINECO through Project No. FIS2014-54734-P and by the Generalitat de Catalunya under Project No. 2014 SGR-581. MZ and PS acknowledge financial support of the Argentinian SECYTUNC and CONICET, as well as support from CCAD Universidad Nacional de Córdoba (Mendieta Cluster) where the molecular dynamics calculations were performed.

[1]M. Zuriaga, L. C. Pardo, P. Lunkenheimer, J. Ll. Tamarit, N. Veglio, M. Barrio, F. J. Bermejo, and A. Loidl, Phys. Rev. Lett. **103**, 075701 (2009).
[2]L. C. Pardo, J. Ll. Tamarit, N. Veglio, F. J. Bermejo, and G. J. Cuello, Phys. Rev. B **76**, 134203 (2007).
[3]Sz. Pothoczki, A. Ottochian, M. Rovira-Esteva, L. C. Pardo, J. Ll. Tamarit, and G. J. Cuello, Phys. Rev. B **85**, 014202 (2012).
[4]J. Reuter, D. Büsing, J. Ll. Tamarit, and A. Würflinger, J. Mater. Chem. **7**, 41–46 (1997).
[5]M. Romanini, Ph. Negrier, J. Ll. Tamarit, S. Capaccioli, M. Barrio, L. C. Pardo, and D. Mondieig, Phys. Rev. B **85**, 134201 (2012).
[6]R. Macovez, A. Goldoni, L. Petaccia, P. A. Brühwiler, and P. Rudolf, Phys. Rev. Lett. **101**, 236403 (2008).
[7]G. Vdovichenko, A. Krivchikov, O. Korolyuk, J. Ll. Tamarit, L. C. Pardo, M. Rovira-Esteva, F. J. Bermejo, M. Hassaine, and M. Ramos, J. Chem. Phys. **143**, 084510 (2015).
[8]M. Rovira-Esteva, N. A. Murugan, L. C. Pardo, S. Busch, J. Ll. Tamarit, Sz. Pothoczki, G. J. Cuello, and F. J. Bermejo, Phys. Rev. B **84**, 064202 (2011).
[9]Ph. Negrier, M. Barrio, J. Ll. Tamarit, and D. Mondieig, Cryst. Growth Des. **13**, 782–791 (2013).
[10]M. Zachariah, M. Romanini, P. Tripathi, M. Barrio, J. Ll. Tamarit, and R. Macovez, J. Phys. Chem. C **119**, 27298–27306 (2015).
[11]R. Brand, P. Lunkenheimer, and A. Loidl, J. Chem. Phys. **116**, 10386–10401 (2002).
[12]M. Romanini, J. C. Martinez-Garcia, J. Ll. Tamarit, S. J. Rzoska, M. Barrio, L. C. Pardo, and A. Drozd-Rzoska, J. Chem. Phys. **131**, 184504 (2009).
[13]A. Criado, M. Jiménez-Ruiz, C. Cabrillo, F. J. Bermejo, R. Fernández-Perea, H. E. Fischer, and F. R. Trouw, Phys. Rev. B **61**, 12082–12093 (2000).
[14]M. Zachariah, M. Romanini, P. Tripathi, J. Ll. Tamarit, and R. Macovez, Phys. Chem. Chem. Phys. **17**, 16053–16057 (2015).
[15]M. Bujak, D. Blaser, A. Katrusiak, and R. Boese, Chem. Commun. **47**, 8769–8771 (2011).
[16]P. Negrier, M. Barrio, J. Ll. Tamarit, D. Mondieig, M. J. Zuriaga, and S. C. Per.ez, Cryst. Growth Des **13**, 2143–2148 (2013).
[17]J. P. Zietlow, F. F. Cleveland, and A. G. Meister, J. Chem. Phys. **24**, 142–146 (1955).
[18]S. C. Pérez, M. Zuriaga, P. Serra, A. Wolfenson, Ph. Negrier, and J. Ll. Tamarit, J. Chem. Phys. **143**, 134502 (2015).
[19]M. Bujak and A. Katrusiak, Z. Kristallogr. **219**, 669–674 (2004).
[20]K. S. Cole and R. H. Cole, J. Chem. Phys. **9**, 341–352 (1941).
[21]K. S. Cole and R. H. Cole, J. Chem. Phys. **10**, 98–105 (1942).
[22]C. Caleman, P. J. van Maaren, M. Hong, J. S. Hub, L. T. Costa, and D. van der Spoel, J. Chem. Theory Comput. **8**, 61–74 (2012).
[23]J. Wang, R. M. Wolf, J. W. Caldwell, P. A. Kollman, and D. A. Case, J. Comput. Chem. **25**, 1157–1174 (2004).
[24]W. L. Jorgensen and J. Tirado-Rives, Proc. Natl. Acad. Sci. U. S. A. **102**, 6665–6670 (2005).
[25]D. van der Spoel, P. J. van Maaren, and C. Caleman, Bioinformatics **28**, 752–753 (2012).
[26]B. Hess, C. Kutzner, D. van der Spoel, and E. Lindahl, J. Chem. Theory Comput. **4**, 435–447 (2008).
[27]G. Allen, P. N. Brier, and G. Lane, Trans. Faraday Soc. **63**, 824–832 (1967).
[28]R. J. Abraham and R. Stolevik, Chem. Phys. Lett. **77**, 181–185 (1981).
[29]T. Rydland and R. Stølevik, J. Mol. Struct.: THEOCHEM **105**, 157–168 (1983).
[30]F. Kremer and A. Schönhals, *Broad Band Dielectric Spectroscopy* (Springer, Berlin, 2003).
[31]M. Bujak, M. Podsiadlo, and A. Katrusiak, Chem. Commun. **37**, 4439–4441 (2008).
[32]K. L. Ngai, J. Non-Cryst. Solids **353**, 709–718 (2007).
[33]G. P. Johari and M. Goldstein, J. Chem. Phys. **53**, 2372–2388 (1970).
[34]K. L. Ngai, J. Chem. Phys. **109**, 6982–6994 (1998).
[35]J. Colmenero, A. Arbe, G. Coddens, B. Frick, C. Mijangos, and H. Reinecke, Phys. Rev. Lett. **78**, 1928–1931 (1997).
[36]F. Alvarez, A. Alegra, and J. Colmenero, Phys. Rev. B **44**, 7306–7312 (1991).
[37]F. Alvarez, A. Alegra, and J. Colmenero, Phys. Rev. B **47**, 125–130 (1993).
[38]D. Fragiadakis and C. M. Roland, Phys. Rev. E **88**, 042307 (2013).
[39]S. Capaccioli, M. Paluch, D. Prevosto, Li-Min Wang, and K. L. Ngai, J. Chem. Phys. Lett. **3**, 735–743 (2012).
[40]J. G. Kirkwood, J. Chem. Phys. **7**, 911 (1939).
[41]H. Fröhlich, *Theory of Dielectrics* (Oxford University Press, London, 1958).
[42]J. C. Martinez-Garcia, J. Ll. Tamarit, S. Capaccioli, M. Barrio, N. Veglio, and L. C. Pardo, J. Chem. Phys. **132**, 164516 (2010).